Geologica Acta, Vol.11, Nº 3, September 2013, 311-320
DOI: 10.1344/105.000001872
Available online at www.geologica-acta.com

geologica acta

Lithospheric magnetic mapping of the northern Caribbean region

M. CATALÁN and J. MARTÍN-DÁVILA

Real Instituto y Observatorio de la Armada
San Fernando 1110, Cádiz, Spain
Catalán E-mail: mcatalan@roa.es Martín-Dávila E-mail: mdavila@roa.es
Fax: 956-599366

ABSTRACT

A more complete crustal perspective of the northernmost part of the Venezuela Basin is provided by data from an international public database processed with new geomagnetic models (CM4) together with data from aeromagnetic surveys and from a recent marine cruise in areas offshore Puerto Rico and the Dominican Republic. The magnetic anomaly map set off three main domains: the North Atlantic plate, a narrow zone extending from the Dominican Republic to Puerto Rico-Virgin Islands, and the North Caribbean Plate. We focused mainly on the latter, applying the Euler deconvolution algorithm in the Venezuela Basin. Shallow and middle depth sources (located between 2km and 12km) are inferred to be the dominant sources (85%), while deep sources are located mostly in the Venezuela Basin, and scarcely appear in the Beata and Aves Ridges. We performed 2D+1/2 modeling on an east-west transect, using Bouguer gravity and magnetic anomaly data to derive a more detailed crustal description of the northern part of the Venezuela Basin. The model suggests that in the Caribbean crust, long wavelengths (>200km) are controlled by variations in crustal thickness, whereas the intermediate ones (50-100km) are mainly controlled by variations in their magnetic properties. It also suggests the presence of a local anomalous body located in the east-west transect, between 487km and 560km, displaying a remarkable positive magnetization contrast (0.3 SI) with regard to the rest of the basin. This body shows a slight increase in density (3010kg/m3), and extends from the bottom of the UCL (Underplate Cumulate Layer) to a depth of 7.5km. We correlate it with the volcanic wedge reported by Driscoll and Diebold (1998).

KEYWORDS | **Caribbean plate. Magnetic anomaly. Poisson's theorem. Potential fields.**

INTRODUCTION

The history of the Caribbean Plate is a matter that remains under debate, especially regarding the formation of the Beata Ridge (Mauffret and Leroy, 1997), and the geological meaning of the Muertos Trough (Granja Bruña *et al*., 2010) (Fig. 1A). Moreover, there is very little data available on the magnetic anomaly in the Venezuela Basin and, consequently, its age and spreading history are poorly known. In a study of several aeromagnetic profiles from Project MAGNET, Donnelly (1973) described a series of NE-SW trending linear magnetic anomalies. Unfortunately, the widely spaced nature of the profiles limited the reliability of the correlations and therefore the observed trends. A more detailed marine magnetic survey of the central part of the basin was carried out by R/V Eastward (Watkins and Cavanaugh, 1974), in which a total of 1550 nautical miles of data were collected. The survey

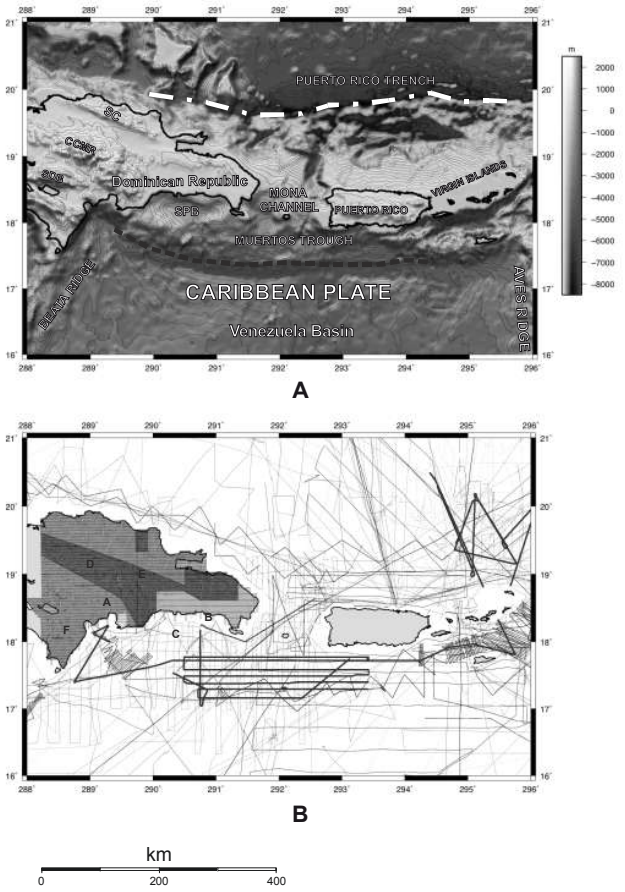

FIGURE 1 | A) Regional framework of the study area. The topographic map is after Smith and Sandwell (1997). Grey palette in meters. Contour interval: 200 meters. CC: Cordillera Central, SC: Cordillera Septentrional, SB: Sierra de Bahoruco, SPB: San Pedro Basin. White dashed-dotted line indicates the Puerto Rico Trench. Black dashed line indicates the Muertos Trough. B) Magnetic surveys used in this paper. Offshore area: GEOPRICO survey in thick black lines. GEODAS data set in thin black lines. On land: the Dominican Republic aeromagnetic flight. A, B, C, D, E and F are the areas surveyed.

comprised seven NW-SE profiles spaced approximately 32km apart. On the basis of these data, Watkins and Cavanaugh were able to identify three separate zones of anomalies: a striped zone over the central area, a smooth or quiet zone towards the southeast, and a short wavelength anomaly zone in the eastern part of the survey area. All these early studies used old geomagnetic models, and most of them were not corrected by external fields.

We contemplated the possibility of using new data from different sources: an international public database, aeromagnetic surveys, and a cruise in the area in 2005. These new data, along with the old data processed with recent geomagnetic models, enabled us to connect onshore and offshore areas, obtaining a more complete crustal perspective of the northernmost part of the Venezuela Basin.

DATA COMPILATION

Magnetic data

Marine data

To carry out this study we used marine magnetic data from the Geophysical Data System (GEODAS) (Metzger and Campagnoli, 2003) gathered from 84 cruises performed in the period between 1960 and 1997. In addition, the Royal Observatory of the Spanish Navy (ROA), in collaboration with other institutions, carried out a geophysical campaign in March-April 2005 in the area (GEOPRICO cruise) (Fig. 1B). Data from all these cruises were scanned to detect and eliminate anomalous readings. In addition, we subtracted the core field contribution for those surveys performed from 1960 to July 2002 using the comprehensive model CM4 (Sabaka *et al*., 2004). This model makes it possible to correct total field marine data through a proper separation of spatial and temporal variations. Crossover analyses were used to estimate the quality of the geophysical surveys, and to provide an effective technique to identify and correct systematic and non-systematic errors in geophysical data grids (Wessel and Watts, 1988; Thakur *et al*., 1999).

We checked the quality of the GEODAS data set by carrying out crossover analyses. Initially, using International Geomagnetic Reference Field (IGRF) models, we obtained a 456nT standard deviation and a 0nT mean value. These values show the heterogeneity of our error sources (secular variation contribution, instrumental precision, etc.). Data from GEOPRICO were corrected by means of lag corrections, spike suppression, and the removal of the external component of the geomagnetic field, using the San Juan Geomagnetic Observatory. To extract the inner field contribution, we used 10th generation IGRF, valid for the period 1900-2010 (Macmillan and Maus, 2005). By applying crossover analysis to GEOPRICO data, we derived 9nT as standard deviation, and 0nT as bias.

GEODAS cruise data were corrected using the CM4 inner field model, and subjected to an empirical correction, provided by the CM4 model, in order to account for the external field contribution.

A careful and detailed analysis of every crossover was performed, discarding those cruises where average residuals were systematically large (we arbitrarily selected 300nT as a threshold). We carried out a leveling on GEODAS track lines, using a statistical tie-line leveling technique (Nelson, 1994), that corrects for intersection errors that follow a specific pattern or trend. The algorithm calculates a least-squares trend line through an error signal to derive a trend error curve, that is then added as a correction to the signal to be leveled. Subsequently, the intersections

between survey lines (from GEOPRICO) and those of the complementary surveys (GEODAS data) were used as tie lines. Finally, this process gave a global precision of 55 nT for the whole GEODAS track line set. We merged both data sets (GEODAS and GEOPRICO) to arrive at a precision of 62nT, that probably reflects some level of incoherency because of the different magnetic models used to extract the core field contribution (CM4 for GEODAS data, and IGRF for GEOPRICO, carried out after 2002, beyond the CM4 period of validation of the model). In order to make proper comparisons with the Dominican Republic's aeromagnetic flight grid (see next sub-section), the magnetic anomaly grid (using GEODAS cruises and GEOPRICO-2005) was upwardly continued to 720m.

Aeromagnetic data

The Dominican Republic's aeromagnetic flight was performed in two phases. The first one was in 1996 and surveyed six blocks (A, B, C, D, E and F), whereas the second was performed in 1999, and surveyed blocks C and D again (Fig. 1B). They used two different along-track distances, 500m and 2000m, depending on the economic interest of the zone. Although the average flight height was 120m, in some areas it was necessary to raise it because of the abrupt topographic relief and safety risks. Additionally, several transversal lines were performed in order to control and increase the quality of the final product. The final grid referred to 720m in height. We merged the marine magnetic data (upwardly continued to 720m) with the aeromagnetic data, obtaining a magnetic anomaly grid with a 2km resolution.

Gravity data

The Gravimetric map (Granja Bruña *et al.*, 2008) was based on two types of data.

Offshore: we used marine gravity data from the GEOPRICO cruise, and satellite-derived gravity data (2 minute-arc, from Smith and Sandwell, 1997). Gravity data in shallow water (200m to 0m) were discarded. Bathymetry was from the ETOPO 2 database (ETOPO, 2001).

Onshore: we used data from the U.S. Geological Survey gravimetric digital map of Puerto Rico (Bawiec, 2001). The Gravity data of the Dominican Republic were obtained by digitizing the Dominican Republic gravity map. Water slab and sea-bottom terrain effects (both on land and at sea) were extracted, using densities of 1.03g/cm^3 and 2.67g/cm^3, respectively. Complete Bouguer anomalies were calculated following the Nettleton (1976) procedure, using a 2km grid and GTOPO 30 data (Gesch *et al.*, 1999) to derive the topographic correction. The final Bouguer anomaly grid had a 5km resolution and was upwardly continued to 720m.

MAGNETIC ANOMALY MAP

From the map we can discern three domains (Fig. 2A): i) the North Atlantic plate; ii) a narrow zone that extends from the Dominican Republic to Puerto Rico-Virgin Islands; and iii) the Caribbean Plate.

The first is located in the northern part; and as Muszala *et al.* (1999) dealt with this zone in great detail, it will not be discussed in the present paper. However, we will highlight its main features, and include them in our map to have a

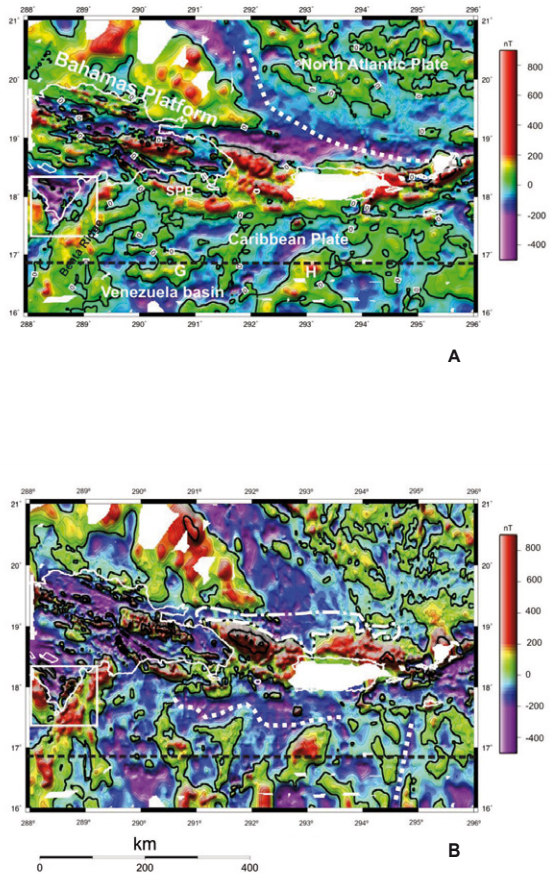

FIGURE 2 | A) Final gridded magnetic anomaly map. G and H mark the magnetic maxima in the North Caribbean Plate. The inserted white square limits the negative magnetic anomaly area (see text for comments). The white dotted line delineates the southern boundary of a slightly positive magnetic anomaly plateau. The black dashed line traces the magnetization density ratio (MDR) profile of Figure 3. SPB: San Pedro Basin. B) Final magnetic grid reduced to the pole. We used 45º and -11.5º as average values for inclination and declination, respectively, for the whole area. The inserted white square limits the negative magnetic anomaly area (see text for comments). The white dotted lines mark the northern and eastern proposed boundaries of the Caribbean plate; the northern boundary roughly corresponds to the Muertos Trough. The dashed-dotted line shows the limit of the extension of the Blueschist belt (according to Muszala *et al.*, 1999). The black dashed line traces the MDR profile of Figure 3 (this profile is modeled in Figure 5). Contour interval: 50nT. The isoline 0nT is plotted in black, coastline in white.

complete representation of the magnetic anomalies in the area. Northwest to southeast trending magnetic highs can be recognized in the northeast sector. A prominent positive magnetic anomaly wedge north of the Dominican Republic shows southeastward trending, and correlates with the Bahamas Platform (Fig. 2A). North of Puerto Rico, we find a slightly positive "plateau" (outlined with dashed white lines in Fig. 2A) that shows positive anomalies to the northwest, interpreted by Muszala *et al*. (1999) as fracture zones.

The second domain, with an east-west arcuate shape, contains the greatest magnetic anomalies in the map (greater than 250nT), particularly in the zone between the Mona Channel and the east of the Virgin Islands (see Fig. 1A for location). North of this high amplitude magnetic anomaly belt, we find an east-west negative anomaly that probably reflects the negative dipolar lobe of the previous cited anomaly. This is confirmed in the map reduced to the pole (Fig. 2B). In the Dominican Republic, a NW-SE set of ribbons can be seen, all of them reflecting a high level of correlation with the local topography (*e.g*. Cordillera Septentrional, Cordillera Central) (Fig. 1A). García-Lobón and Rey-Moral (2004) studied the whole domain using the Dominican Republic aeromagnetic flight and radiometric data, performing a geo-structural cartography of the island. The Sierra de Bahoruco, extending through the meridional side of the Island (Fig. 2A, inside a white square), shows a systematic negative magnetic anomaly area, that the above authors interpreted as caused by a deep paramagnetic body. The map presents a clear dichotomy in this second domain, revealing two different blocks —one comprises the Dominican Republic, and the other extends from the Mona Channel to the Virgin Islands. The latter, characterized by strong positive magnetic anomalies, appears to be fractured in the Mona Channel as well as at San Pedro Basin (Fig. 2A) into two blocks, suggesting left-lateral strike slip between them. This dichotomy could point to the separation of the Dominican Republic and Puerto Rico-Virgin Islands into different tectonic blocks.

The third domain is that of the Caribbean Plate. Here the anomaly map shows a nearly N-S trending high (positive) magnetic anomaly that geographically correlates with the Beata Ridge. The rest of the map shows a local positive magnetic anomaly (G in Fig. 2A), while another positive magnetic anomaly located south of Puerto Rico, with a NE-SW trend, is clearly depicted (H in Fig. 2A).

REDUCTION TO THE POLE MAP

To help further in the interpretation of the magnetic anomaly data of this area, reduction to the pole (RTP) was also applied. This procedure transforms data collected in areas where the magnetic inclination is not vertical into data referring to the geomagnetic pole, positioning them symmetrically over their sources. Reduction to the pole assumes that magnetization is caused only by induction, and needs the magnetic inclination and magnetic declination. We have used 45º as the average values for inclination in the whole area and -11.5º for declination.

The RTP map provides a slightly different picture (Fig. 2B). The whole anomaly set appears to be shifted to the NW, although this offset is lesser in the Caribbean Plate. Further changes can be detected: the Sierra de Bahoruco (Fig. 2B, inside a white square) keeps the minima but seems to be more localized; in the north, the east-west dipolar magnetic anomaly that runs from the Mona Channel to the Virgin Islands is modified in shape and replaced by a high-amplitude anomaly that appears in the north of Puerto Rico. Muszala *et al*. (1999) related it to arc magmatism.

Between the Bahamas Platform and this high-amplitude anomaly belt, a low-amplitude anomaly is depicted (a white dashed-dotted line in Fig. 2B), that Muszala *et al*. (1999) correlated with the extension of a Blueschist belt.

In the Caribbean Sea, a set of linear north-southward magnetic anomalies (east of the Beata Ridge) can be found distributed over a negative terrace. This negative horizon is clearly constrained: in the west, by the Beata Ridge; in the north, by a new low–amplitude east-west anomaly that is identified as the Muertos Trough (Fig. 1A; 2B, white dotted line); and as its easternmost limit we propose a negative north-south anomaly (north-south white dotted line in Fig. 2B). This negative RTP magnetic anomaly terrace suggests that the magnetic rocks causing these anomalies possesses a strong remanent that may be reversed relative to the present field of the Earth. This relatively flat magnetic area indicates intermediate or deep magnetic rocks (probably 6 km of depth or more). This is supported by the small NW shift that experimented the magnetic anomalies once reduced to the pole (Fig. 2A; B).

POISSON'S THEOREM

This theorem establishes a linear relationship between magnetic and gravity potentials, in particular, between the magnetic potential and the gravitational attraction component in the direction of magnetization, provided that three conditions are met: i) the sources generating the magnetic and the gravity potentials are the same, ii) the direction of magnetization is uniform within the sources, and iii) the magnetization-density ratio (MDR) is constant within the sources (Blakely, 1995).

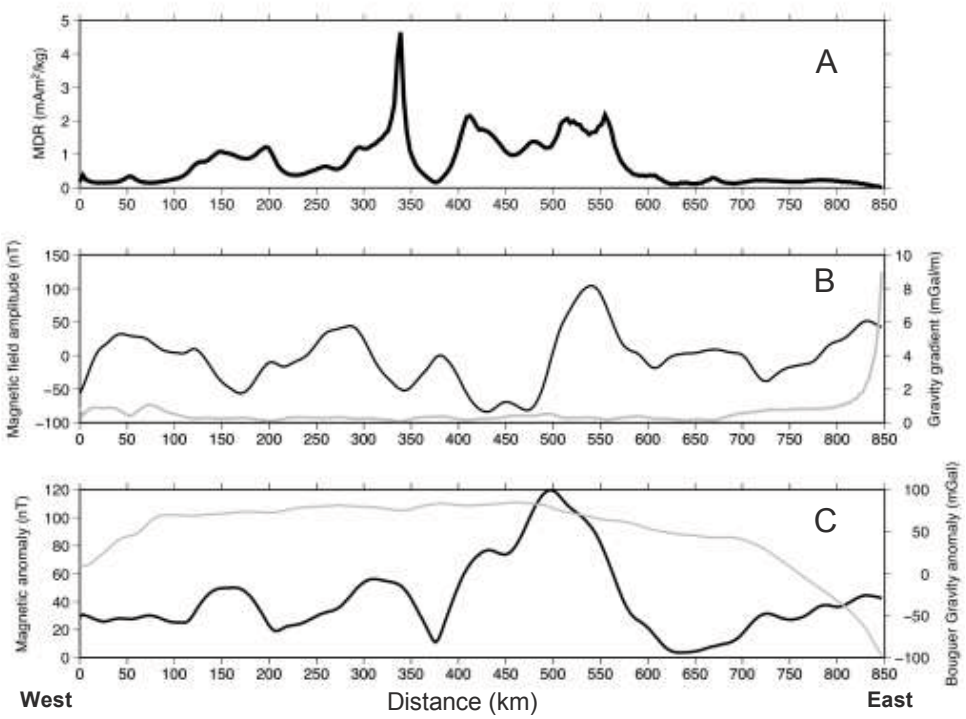

FIGURE 3 | MDR profile (see Figure 2 for location). A) MDR values. B) Magnetic field amplitudes (black line) and gravity gradients (grey line), in nT and mGal/km, respectively. C) Magnetic anomaly (black line) and Bouguer gravity anomaly (grey line), in nT and mGal, respectively. Both gravity and magnetic data were upwardly continued to 10 km above sea level (see text for comments).

Poisson's theorem has been used in the past to calculate single-source magnetization-density ratios (Garland 1951; Kanasewich and Agarwal, 1970) and the direction of source magnetization (Ross and Lavin, 1966; Cordell and Taylor, 1971). Chandler *et al*. (1981) extended its use to multi-source data by repeatedly applying the theorem within a small moving data window. Its size involved interplay between the number of data points necessary to achieve a credible linear regression (lower limit) and the interference from neighboring anomalies (upper limit). Chandler and Malek (1991) applied this technique to a complex Precambrian geological region in central Minnesota that contained complex interfering anomalies. Three parameters –the correlation coefficient, slope and intercept – were generated at each data interval, to reflect the internal correlation existing between gravity and magnetic anomalies and possibly yield information regarding anomaly source properties. The slope parameter provided an estimate of the source magnetization-to-density ratio for the anomaly segments within each window position.

POISSON'S THEOREM APPLIED TO THE NORTHERN CARIBBEAN SEA

Mendonça (2004) proposed a simple analytical technique whereby both the MDR and magnetization direction (MI) could be derived automatically in a one-step process (non-iterative) from a pair of gravity and magnetic profiles in those regions where Poisson's conditions were satisfied. This method constitutes an objective tool for analyzing the magnetization and density of the northern Caribbean Sea. Our idea was to apply this algorithm on an east-west profile running along the northern part of the Caribbean Sea (Fig. 2 for location), to use it as a physical profiler, inferring information about variations in density and magnetization useful to further constrain the 2+1/2D gravity and magnetic modeling (see section Gravity and magnetic modeling).

The processing routine incorporates a step where space derivatives are calculated (Mendonça, 2004). In order to prevent excessive noise amplification during these mathematical operations, both gravity and magnetic data were upwardly continued to 10km above sea level. To select the height, some tests were conducted until MDR short wavelength disturbances (not related with geological features) disappeared.

Figure 3A shows three different MDR zones: i) a low MDR amplitude zone that reaches 96km in horizontal distance, and presents an average value of 0.19±0.05mA·m^2/kg in its easternmost part; ii) a zone that goes from 134km to 573km, where the MDR fluctuates up and down and presents the greatest value (1.09±0.66mA·m^2/kg) on average in the profile; and iii) a zone that goes from 600km to the end of

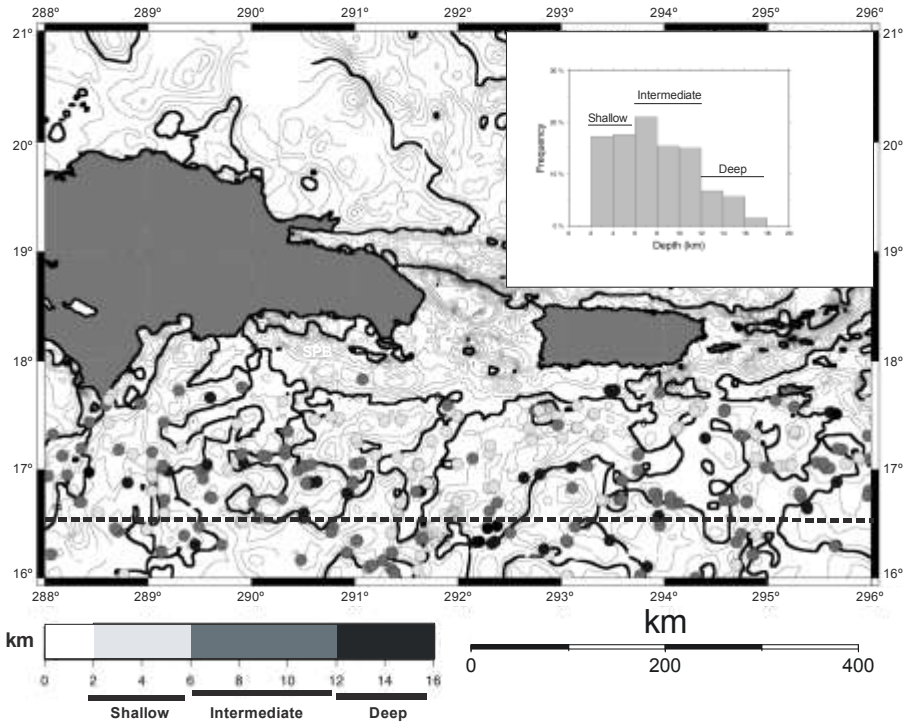

FIGURE 4 | Euler solutions overlying the contour scalar magnetic map for a structural index (SI) of 2.5 and a depth tolerance of 15%. Inserted histogram with a depth estimation of the centroid's causative body location (see text for comments). Contour interval: 50nT. The isoline 0nT is plotted in black. The black dashed line traces the MDR profile of Figure 3 (this profile is modeled in Fig. 5). SPB: San Pedro Basin.

the profile, where the MDR presents very small amplitude values (0.18±0.04mA·m²/kg). Additionally, an MDR peak appears at 338km. As the Bouguer gravity anomaly profile (Fig. 3C) shows quite uniform behavior in this zone, it is interpreted not as a violation of Poisson's conditions but rather as an area where magnetization becomes stronger than in the immediate eastern surroundings. This aspect will be discussed in the Gravity and Magnetic modeling section.

Special attention should be paid to the Bouguer gravity anomaly values (thick grey line in Fig. 3C). Three main domains are seen along the profile: a western, a central and an eastern domain. The westernmost and easternmost parts of the profile respectively display increasing and decreasing trends, while the central domain shows a stable or uniform behavior. We interpreted it to be caused by variations in crustal thickness. In particular, the westernmost part is linked with the Beata Ridge, while the easternmost part is linked with the Aves Ridge. Both these zones present a thicker crust, according to seismic refraction studies (Edgar *et al.*, 1971; Boynton *et al.*, 1979). The central domain crust, though less thick, is considered anomalously thick for purely oceanic crust (Burke *et al.*, 1978; Diebold *et al.*, 1981).

The magnetic anomaly profile (thick black line in Fig. 3C) shows a short wavelength, and the magnetic field gradient (thick black line in Fig. 3B) shows a strong correlation with the MDR variation. This led us to propose that in the Caribbean crust, longer wavelengths (longer than 200km) are controlled by variations in crustal thickness, while the intermediate wavelengths (50-100m) are mainly controlled by variations in their magnetic properties. The 2+1/2D model would confirm this notion.

It is important to emphasize that a crustal thickening (as in the Beata and Aves Ridges) justifies a weakening in the average density, and should cause an increase in MDR, yet we obtain lesser values there. Thus, we deduce that the main local contribution to its geological identity would be magnetization.

EULER DECONVOLUTION

We applied the Euler deconvolution algorithm (Thomson, 1982; Reid *et al.*, 1990) to the magnetic anomaly grid (Fig. 4) to enhance the modeling. The Euler equation relates the magnetic (or gravity) field and its gradients, and the location of the source to the degree of homogeneity N, which may be interpreted as a Structural Index (SI) (Thomson, 1982). This index quantifies a field´s rate of change with distance. Our magnetic anomaly map (Fig. 2A) shows short wavelength anomalies at the Venezuela Basin, limited in the horizontal plane, and

TABLE 1 | Physical properties used in gravity and magnetic model

	L (m)	g (m/s^2)	ρ (Kg/m^3)	μ (Pa.s)	V (m/s)	t (s)	σ (Pa)
Nature	1000	9.81	2300	2×10^{18}	1.6×10^{-10} (0.5 cm/y)	3.2×10^{13} (1 Ma)	2.3×10^{6}
Model	0.01	9.81	1400	3.5×10^{4}	5.6×10^{-6} (2 cm/y)	9.2×10^{3} (2.5 h)	14
Model/Nature Ratio	10^{-5}	1	0.6	1.8×10^{-15}	3.5×10^{4}	2.9×10^{-10}	6×10^{-6}

inevitably in the vertical, suggesting a high SI. An index of 3 would represent the ideal body, that is, a sphere. Index 2 could indicate a body with one infinite dimension. We believe this is an intermediate case, best reflected by an index of 2.5 (Reid *et al.*, 1990). As they were conditioned by the SI selection, all depths should not be considered accurate data, but rather as an estimation of the centroid's causative body location. Figure 4 shows our set of Euler solutions after filtering out all solutions that fell beyond the Venezuela Basin. We recognized three different depth segments (Fig. 4): i) shallow sources (depths from 2km to 6km); ii) intermediate depth sources (depths from 6km to 12km); and iii) deep sources (depths from 12km to 18km). The shallow sources hold 34% of the Euler solution set; intermediate depth sources concentrate almost 51% (note that the segment 6km to 8km depth contains the most solutions, nearly 22%), and deep sources concentrate 13%. Figure 4 also shows their geographical location.

We may conclude that: i) shallow and intermediate depth sources appear to predominate (almost 85%); and ii) deep sources are located mainly in the Venezuela Basin, and scarcely appear on the Beata and Aves Ridges. This information was used to constrain our 2D+1/2 model.

GRAVITY AND MAGNETIC MODELING

To model the MDR profile, magnetic models were executed in 2+1/2D (Talwani and Heirtzler, 1964; Campbell, 1983), and Bouguer anomaly values were used as gravity data.

Because of the controversial origin of the Venezuela Basin, for the gravimetric and magnetic modeling we defined a 4-layer crust, following and slightly modifying Mann and Burke (1984). The first layer is the sedimentary layer, the second is the oceanic Layer 2, the third is oceanic Layer 3, and the fourth, that provides extra crustal thickness through underplating processes, is referred to as the Underplate Cumulate Layer (UCL). These processes could have affected Layer 3, modifying its previous "normal" oceanic lithology and/or thickening it. Layer composition (density and bulk susceptibility) is shown in Table I.

Although the fit to the observed gravity is excellent, we did not attempt to fit the details of the composite magnetic profile except to, approximately, reproduce the observed wavelengths and amplitudes.

As previously mentioned, the gravity model shows a uniform behaviour throughout the basin. A great wavelength is displayed, showing a gravity high (300mGal) in the middle of the basin. Additionally, short wavelength signals (10 to 20mGal amplitude) are accommodated by modifying Layer 3 and UCL thickness as well.

The top of Layer 2 is at a depth of 4.5km, and its bottom at 6.5km on average. The bottom of Layer 3 is 8.5km deep on average, and the layer thickness varies, being almost absent in some areas (*i.e.* between 248km to 291km). The UCL has its bottom at 12km, becoming thinner (bottom at 10.5km) from 355km to 500km. Its top accommodates most of the Layer 3 thickness variation.

Concerning magnetic modeling, sediments were considered to have null total magnetization. The UCL and mantle were considered non-magnetic, taking into account thermal gradient effects.

We initially adjusted the magnetic model by only modifying the bulk susceptibility and thickness of Layers 2 and 3. The best fit was obtained by giving a positive susceptibility contrast of 0.04 IS to Layer 2 between its western and its eastern part. Nevertheless, as we pursue the simplest solution, and it seems difficult to justify this dichotomy in magnetization on our fit, we arbitrarily neglect it. Our magnetic fit precision worsens from 32nT to 37nT rms, which seems acceptable. The Euler solution set additionally shows that the magnetic contribution is greater when based on intermediate/deep sources in the area (Fig. 4).

Concerning the Beata Ridge and the westernmost part of the Aves Ridge, Euler solutions (Fig. 4) provide shallower, and scarcely deep sources. This leads us to consider a simplistic assumption: their upper crust as the only magnetic contributor. We fitted these two edge areas by modifying the upper crust magnetization, that seems to show a sharp positive contrast value (0.1 SI difference) as opposed to the non-magnetic character of Layer 2 in the rest of the basin.

An anomalous body located between 487 km to 560km shows a remarkable positive magnetization contrast (0.3SI)

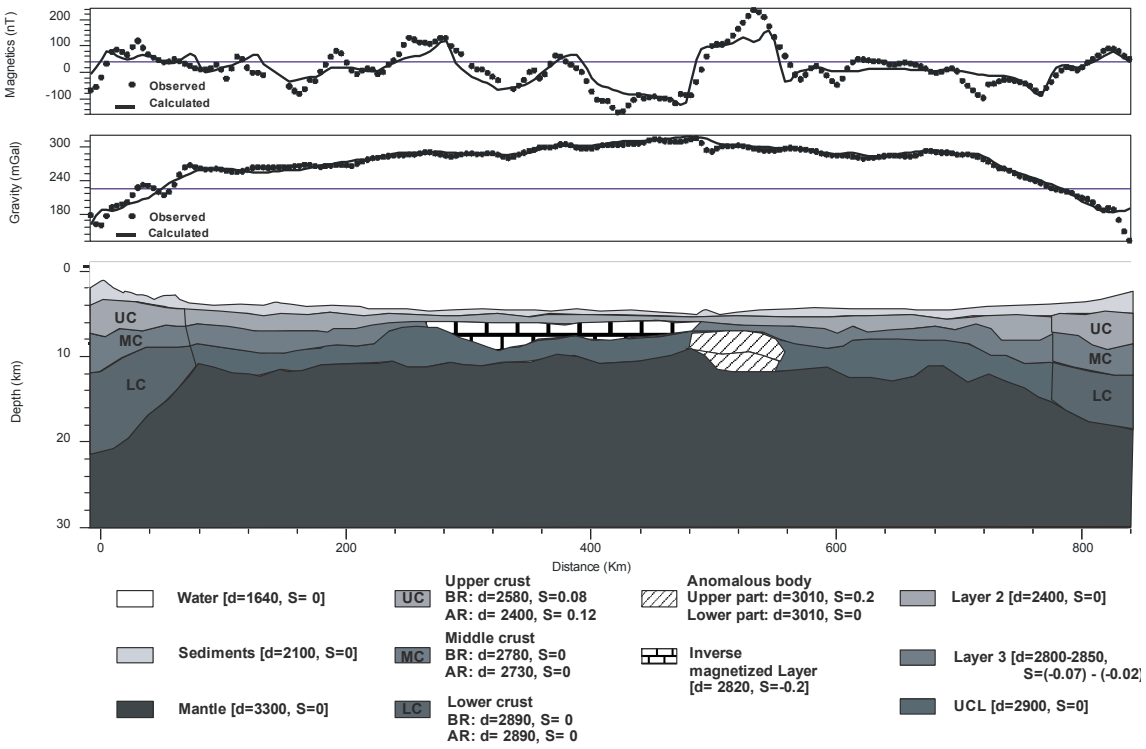

FIGURE 5 | Magnetic and gravity models for the east-west profile. Magnetic units: nT. Gravity units: mGal. Susceptibility units: S.I.. Density units: kg/m^3. Profile location is shown in Figure 2. BR: Beata Ridge. AR: Aves Ridge. UC: Upper crust. MC: Middle crust. LC: Lower crust. UCL: Underplate Cumulate Layer.

with regard to the Venezuela Basin. This deep body shows a slight increase in density (3010kg/m^3), and although it extends from the bottom of the UCL to a depth of 7.5km, taking into account thermal effects we arbitrarily consider it to be non-magnetic in its deepest level (Fig. 5). We correlate it with the volcanic wedge reported by Driscoll and Diebold (1998).

Layer 3 shows a negative susceptibility value (-0.07 to -0.02). It could explain the first MDR zone (from 134 km to 500km) where the MDR presents the greatest average value for the profile (mA·m^2/kg). Moreover, it is worth emphasizing that the proposed model suggests an enhancement of this inverse magnetization, as seen in Figure 5: from -0.02/-0.07SI interval at Layer 3 to -0.2SI at the inverse magnetized Layer, from 290km to 500km at Layer 3 depth. The latter limit could be extended to 560km, but as there is a strong deep magnetic source in this area, is difficult to determine the eastern limit.

This inverse magnetization shows the importance of the remanent magnetization in the whole northern Venezuela Basin, and is consistent with the extensive basaltic sills and flow episodes that may have disturbed and destroyed any previous magnetic anomaly pattern (Burke *et al.*, 1978; Diebold *et al.*, 1981).

The thickness variation of this inverse magnetized Layer would explain the MDR profile from 290km to 520km: high MDR values are interpreted in the 2+1/2D model as a thickening of an inverse magnetized body (at Layer 3), while a decrease in the MDR plot is interpreted in opposite terms.

The two ends of the profile, the Beata and Aves Ridges, show different vertical crustal structures that explain the low Bouguer anomaly values. Note that a weakening in the Bouguer gravity anomaly values maybe linked with a stronger MDR amplitude. However, we find the lowest MDR amplitude values in this area, which is only compatible with a dropping off of magnetic properties. This is confirmed by the bulk susceptibility contrast that highlights the middle crust. As stated before, the model suggests a contrast of nearly 0.1SI between the Beata and Aves Ridges' upper crust and the rest of the Venezuela Basin.

CONCLUSIONS

The use of data from international public databases processed with new geomagnetic models (CM4) together with data from aeromagnetic surveys and from a recent cruise (2005) in the area enable us to more properly connect onshore and offshore areas, obtaining a more complete crustal perspective of the northernmost part of the Venezuela Basin.

From the magnetic anomaly map (Fig. 2A) we can recognize three domains: i) the North Atlantic Plate; ii) a high amplitude narrow zone, that extends from the Dominican Republic to Puerto Rico-Virgin Islands; and iii) the Caribbean Plate. Particularly, the map presents a clear dichotomy between the Dominican Republic and Puerto Rico-Virgin Islands, delineating two different blocks. They appear to be fractured in the Mona Channel as well as at San Pedro Basin suggesting a left-lateral strike slip between them (Fig. 4). This dichotomy suggests the separation of the Dominican Republic and Puerto Rico-Virgin Islands into different tectonic blocks.

Application of the Euler deconvolution algorithm in the Venezuela Basin led us to identify three different segments (inserted graph in Fig. 4): i) shallow sources (2km to 6km); ii) intermediate depth sources (6km to 12km); and iii) deep sources (12km to 18 km). Additionally, we can infer that the shallow and middle depths are the dominant sources (85%) and that deep sources are located mainly in the Venezuela Basin and scarcely appear on the Beata and Aves Ridges.

In order to have a detailed crustal description of the area, we performed a 2D+1/2 model of an east-west transect. This profile runs from the westernmost part of Venezuela Basin (Beata Ridge) to its easternmost part (Aves Ridge). Our model fitted Bouguer gravity as well as magnetic anomaly data. Furthermore, we obtained an MDR profile by applying a Poisson theorem-based algorithm.

A 4-layer crust was defined. The first layer behaves as sediment, the second and third as oceanic Layers 2 and 3, respectively, and the fourth (UCL), that provides the extra crustal thickness, is interpreted as formed by underplating processes.

We considered the sedimentary layer, the UCL and the mantle to be non-magnetic, taking into account thermal gradient effects, and adjusted the magnetic model by controlling the bulk susceptibility and thickness of Layer 3.

The model suggests that the longer wavelengths (>200km) in the Caribbean crust are controlled by variations in crustal thickness, whereas the intermediate ones (50-100km) are mainly controlled by variations in their magnetic properties.

The proposed model suggests the presence of an inverse magnetized body in Layer 3 that extends from 290km to 500km, inserted in the east-west transect. Additionally, a local anomalous body that shows a remarkable positive magnetization contrast (0.3SI) with regard to the rest of the basin is located between 487km and 560km. This body shows a slight increase in density (3010kg/m^3) and extends upwards from the bottom of the UCL to a depth of 7.5km. We correlate it with the volcanic wedge reported by Driscoll and Diebold (1998).

ACKNOWLEDGMENTS

All figures were done using GMT software (Wessel, 1989; Wessel and Smith, 1998). We are indebted to Dr. Alfonso Muñoz and to Dirección General de Minería for providing us with the Bouguer gravity grid and the Dominican Republic aeromagnetic data, respectively. We thank the captain and crew of the research vessel "Hespérides" as well as the GEOPRICO Working Group, and the technicians from the Unidad de Tecnología Marina (Spanish National Research Council).

REFERENCES

Bawiec, W.J., 1999. Geology, Geochemistry, Geophysics, Mineral Occurrences and Mineral Resource Assessment for the Commonwealth of Puerto Rico. U.S. Geological Survey, Open-file Report, 98, 38.

Boynton, C.H., Westbrook, G.K., Bott, M.H.P., Long, R.E., 1979. A seismic refraction investigation of crustal structure beneath the Lesser Antilles Island Arc. Royal Astronomical Society Geophysics Journal, 58, 371-393.

Burke, K., Fox, P.J., Sengör, A.M.C., 1978. Buoyant ocean floor and the evolution of the Caribbean. Journal of Geophysical Research, 83, 3949-3954.

Campbell, D.L., 1983. Basic programs to calculate gravity and magnetic anomalies for 2+1/2 dimensional prismatic bodies. U.S.Geological Survey, Open-file Report 83-154.

Cordell, L., Taylor, P.T., 1971. Investigation of magnetization and density of a North American seamount using Poisson's theorem. Geophysics, 36(5), 51-62.

Chandler, V.W., Koski, J.S., Hinze W.J., Braille, L.W., 1981. Analysis of multi-source gravity and magnetic anomaly datasets by moving-window application of Poisson theorem. Geophysics, 46(1), 30-39.

Chandler, V.W., Malek, K.C., 1991. Moving-window Poisson analysis of gravity and magnetic data from the Penokean orogen, east central Minnesota. Geophysics, 56(1), 123-132.

Diebold, J.P., Stoffa, P.L., Buhl, P., Truchan, M., 1981.Venezuela Basin crustal structure. Journal of Geophysical Research, 86, 7901-7923.

Donnely, T.W., Melson, W., Kay, R., Rogers, J.J.W., 1973. Basalts and dolerites of Late Cretaceous age from the central Caribbean. In: Edgar, N.T. and others (eds.). Initial Reports of the Deep Sea Drilling Project, Washington, D.C., U.S. Government Printing Office, 15, 989-1011.

Driscoll, N.D., Diebold, J.B., 1998. Deformation of the Caribbean region: One plate or two? Geology, 26, 1043-1046.

ETOPO-2 (World Data Center for Marine Geology and Geophysics: 2-minute gridded global relief data), 2001.

National Geophysical Center (NGDC), NOAA Satellite and Information Service. Website: http://www.ngdc.noaa.gov/mgg/fliers/01mgg04.html .

García-Lobón, J.L., Rey-Moral, C., 2004. Magnetismo y radiación gamma natural de la República Dominicana. Boletín Geológico y Minero, 115(1), 153-168.

Garland, G.D., 1951. Combined analysis of gravity and magnetic anomalies. Geophysics, 16, 51-62.

Gesch, D.B., Verdin, K.L.,Greenlee, S.K., 1999. New land surface digital elevation model covers the earth. Eos, Transactions, American Geophysical Union, 80, 69-70.

Granja Bruña, J.L., Carbó-Gorosabel, A., Muñoz-Martín, A., Llanes Estrada, P., 2008. Gravity maps in the northeastern Caribbean Plate boundary zone. Santo Domingo (Dominican Republic), Transactions of the 18th Caribbean Geological Conference, 27, 48.

Granja Bruña, J.L., Muñoz-Martín, A., ten Brink, U., Carbó-Gorosabel, A., Llanes Estrada, P., Martín-Dávila, J., Córdoba-Barba, D., Catalán Morollón, M., 2010. Gravity modeling of the Muertos Trough and tectonic implications (north eastern Caribbean). Marine Geophysical Reseraches, 31, 263-283. DOI: 10.1007/s11001-010-9107-8

Kanasewich, E.R., Agarwal, R.G., 1970. Analysis of combined gravity and magnetic fields in wave number domain. Journal of Geophysical Research, 75, 5702-5712.

Macmillan S., Maus, S., 2005, International Geomagnetic Reference Field - The 10th-Generation. Earth Planets Space, 57, 1135-1140.

Mann, P., Burke, K., 1984. Neotectonics of the Caribbean. Reviews of Geophysics and Space Physics, 22(4), 309-362.

Mauffret, A., Leroy, S., 1997. Seismic stratigraphy and structure of the Caribbean Sea. Tectonophysics, 283, 61-104.

Mendonça C.A., 2004. Automatic determination of the magnetization-density ratio and magnetization inclination from the joint interpretation of 2D gravity and magnetic anomalies. Geophysics, 69(4), 938-948.

Metzger, D., Campagnoli, J., 2007. Marine Trackline Geophysics Data on DVD, version 5.0.10, NOAA, National Geophysical Data Center.

Muszala, S.P., Grindlay, N.R., Bird, R.T., 1999. Three-dimensional Euler deconvolution and tectonic interpretation of marine magnetic anomaly data in the Puerto Rico trench. Journal Geophysical Research, 104, 29175-29187.

Nelson, J.B., 1994. Leveling total-field aeromagnetic data with measured horizontal gradient. Geophysics, 59, 1166-1170.

Nettleton, L.L., 1976. Gravity and magnetics in oil exploration. New York, McGraw-Hill, 464pp.

Reid, A.B., Allsop, J.M., Granser, H., Millet, A.J., Somerton, I.W., 1990. Magnetic interpretation in three dimensions using Euler deconvolution. Geophysics, 55(1), 80-91.

Ross, H. P., Lavin, P.M., 1966. In-situ determination of the remnant magnetic vector of two dimensional tabular bodies. Geophysics, 31(5), 949-962.

Sabaka, T., Olsen, N., Purucker, M., 2004. Extending comprehensive models of the earth's magnetic field with Oersted and CHAMP data. Geophysical Journal International, 159, 521-547.

Sandwell, D.T., Smith, W.H.F., 1997. Marine Gravity from Geosat and ERS-1 Altimetry. Journal Geophysical Research, 102, 10039-10054.

Smith, W.H.F., Sandwell, D.T., 1997. Global seafloor topography from satellite altimetry and ship depth soundings. Science, 277, 1956-1962.

Talwani, M., Heirtzler, J.R., 1964. Computation of magnetic anomalies caused by two-dimensional structures of arbitrary shape. In: Parkes, G.A. (ed.). Computers in he mineral industries. Stanford, CA, University Publications, Geological Sciences, 9, 464-480.

Thakur, N.K., Gangadhara Rao, T., Subrahmanyam, C., Khanna, R., 1999. Crossover analysis of geophysical data in Bay of Bengal. Geo-Marine Letters, 19, 262-269.

Thomson, D.T., 1982. EULDPH: A new technique for making computer-assisted depth estimates from magnetic data. Geophysics, 55, 80-91.

Watkins, J., Cavanaugh, T., 1974. Implications of magnetic anomalies in the Venezuelan Basin. Guadaloupe, Transactions of the VII Caribbean Geological Conference, 129-138.

Wessel, P., Watts, A.B., 1988. On the accuracy of marine gravity measurements. Journal Geophysical Research, 93, 393-413.

Wessel, P., Smith, W., 1998. New, improved version of generic mapping tools released. EOS, Transaction American Geophysical Union, 79(47), 579.

Manuscript received June 2011;
revision accepted November 2012;
published Online June 2013.

ELECTRONIC APPENDIX

TABLE I | Physical properties used in gravity and magnetic model

Unit		Density (kg/m^3)	Susceptibility (SI)
Sea water		1640	0
Sedimentary Layer		2100	0
Layer 2		2400	0
Layer 3		2800-2850	(-0.07) □(-0.02)
Inverse magnetized Layer		2800	-0.2
Underplate Cummulates Layer (UCL)		2900	0
Mantle		3300	0
Anomalous body		3010	0.2
Beata Ridge	Upper crust	2580	0.08
	Middle crust	2780	0
	Lower crust	2892	0
Aves Ridge	Upper crust	2500	0.12
	Middle crust	2730	0
	Lower crust	2890	0